



Relating grain size to the Zener–Hollomon parameter for twin-roll-cast AZ31B alloy refined by friction stir processing

A.H. Ammouri^a, G. Kridli^b, G. Ayoub^{c,d}, R.F. Hamade^{d,*}

^a Department of Industrial and Mechanical Engineering, Lebanese American University, Byblos, Lebanon

^b Industrial and Manufacturing Systems Engineering, University of Michigan-Dearborn, Dearborn, MI, United States

^c Department of Mechanical Engineering, Texas A&M University at Qatar, Doha, Qatar

^d Department of Mechanical Engineering, American University of Beirut, Beirut, Lebanon

ARTICLE INFO

Article history:

Received 9 September 2014

Received in revised form 24 January 2015

Accepted 27 February 2015

Available online 23 March 2015

Keywords:

Twin-roll-cast AZ31B

Friction stir processing

Dynamic recrystallization

Zener–Hollomon parameter

ABSTRACT

An experimentally verified finite element model was used to estimate the strain rate and the temperature values which were, consequently, used in calculating the Zener–Hollomon parameter, Z-parameter, of twin-roll-cast (TRC) AZ31B after being refined by FSP (using range of spindle speeds of 600–2000 rpm and tool feed rates ranging from 75 to 900 mm/min). In the finite element model, an HCP specific Zerilli–Armstrong constitutive relation was used to describe the mechanical behavior of AZ31B. The resulting grain size values were experimentally measured for the observed microstructure of all processed samples. Dynamic recrystallization was identified to be the main mechanism involved in the grain refinement. A linear relation of the form $\ln d = a \times \ln Z + b$ was determined relating the average grain size (d) to the Z-parameter with a and b being equal to -0.23 and 8.79 , respectively. These coefficients differed from values reported by others for AZ31 magnesium alloy with this difference being attributed to different material processing techniques used in the as-received condition. The resulting equation can be used in controlling the grain size during friction stir processing by varying the process parameters (spindle speed and tool feed) that would in turn affect the instantaneous value of the Zener–Hollomon parameter.

© 2015 Elsevier B.V. All rights reserved.

1. Introduction

Magnesium alloys are known to be the lightest structural metal in use nowadays, with a high specific strength those materials are of high interest particularly in the transportation industry (Friedrich and Schumann, 2001). Sheet forming techniques are often used to produce product components for several industries including aerospace and automotive. Magnesium alloys exhibit low formability at room temperature but can be generally improved through material processing techniques producing fine grained microstructure.

Friction stir processing (FSP) is a microstructure-modifying process that has been under continuous development since its introduction in 2001 (Mishra and Mahoney, 2001). The combination between severe mechanical deformations and frictional heating associated with FSP is believed to trigger grain refinement, resulting in materials with improved mechanical properties. Darras et al. (2007) and Chang et al. (2007) studied the effect of

evolving the FSP process parameters on the resultant grain size. Ultrafine-grained microstructures with average grain size as small as 100–300 nm were achieved. An investigation by Chang et al. (2008) demonstrated the capacity of the process to achieve an average grain size of 85 nm by two-pass FSP.

The Zener–Hollomon parameter (Z-parameter), a temperature compensated strain rate, is defined as $Z = \dot{\epsilon} \exp(Q/RT)$ in terms of strain rate ($\dot{\epsilon}$) and temperature (T) with universal gas constant ($R = 8.314 \text{ J/K mol}$), and activation energy ($Q = 130 \text{ kJ/mol}$ (McQueen et al., 2000)). Z-Parameter has been (Wang et al., 2003) related to resulting grain size due to dynamic recrystallization (DRX) in extruded magnesium-based alloys. A relationship between the Z-parameter and the average recrystallized grain size for extruded (not twin-roll cast) AZ31B plates during FSP was established by Chang et al. (2004) the coefficients of which were found to be different from those obtained earlier by Wang et al. (2003). In Darras (2008), slightly different coefficients for AZ31B-O (annealed) sheets were also determined experimentally for conditions similar to those used during FSP. Given that to the authors' best knowledge no relation has been previously published relating the Z-parameter to the resulting grain size of friction stir processed TRC AZ31B, the authors in this work aim to determine the coefficients of such a

* Corresponding author. Tel.: +961 1350000x3481.
E-mail address: rh13@aub.edu.lb (R.F. Hamade).

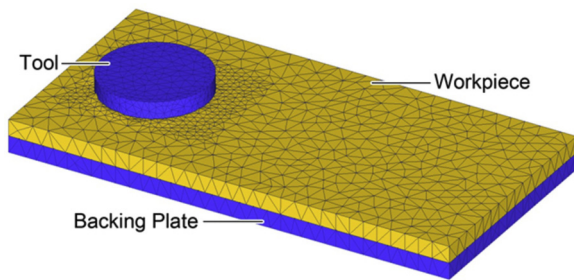


Fig. 1. The meshed FEM model used in the simulations.

relation. To this end, a test matrix comprised of different ranges of FSP process parameters of spindle speed and feed rate was run and the resulting grain (d) size of the processed material was measured using optical microscopy. For the same process parameters, an experimentally validated FE model (Ammouri et al., 2013) was used to determine the strain rates and temperatures during FSP which are needed to calculate the values of the corresponding values of the Z-parameter. Linear regression was used to determine the coefficients of the relation between the average grain size and the Z-parameter.

Controlling grain size in friction stir processes can be achieved by utilizing the proposed relation in the control system of the friction stir processing machine tool along with other relations that would relate the Z-parameter to FSP's process parameters. The equation can be used in open loop control mode by selecting a desired grain size and calculating the corresponding required processing parameters. For more accurate control and to account for process variations, this equation can be used in a closed loop control system that monitors the temperature of the process and update the process parameters accordingly. This however would require further equations that relate the process temperature to the process parameters.

2. Finite element simulations

In this section, reported are the details of the finite elements model, the constitutive equation used to represent the mechanical behavior of AZ31B, and the results of the FE model.

2.1. The FEE model

The 3D thermo-mechanically coupled FE model in this work was developed by the authors (Ammouri et al., 2013) using the commercial FEA software DEFORM-3D™ (SFTC, 2545 Farmers Drive, Suite 200, Columbus, Ohio). The 3D model consists of the FSP tool, the workpiece, and the backing plate as shown in Fig. 1.

Both the tool and the backing plate were modeled as rigid undeformable bodies and were meshed to account for heat transfer only. The workpiece was modeled as a plastic body subject to both deformation and heat transfer. (Detailed description of the FE model can be found in Ammouri et al. (2013) and Ammouri and Hamade (2013a).)

2.2. The material constitutive equation

An HCP specific Zerilli–Armstrong (ZA) constitutive relation, based on thermally activated dislocation mechanics, was used to model the flow stress of the magnesium workpiece according to Zerilli (2004):

$$\sigma = C_0 + B \exp(-(\beta_0 - \beta_1 \ln \dot{\varepsilon})T) + B_0 \sqrt{\varepsilon_r} \left(1 - \exp\left(-\frac{\varepsilon}{\varepsilon_r}\right)\right) \exp(-(a_0 - g\alpha_1 \ln \dot{\varepsilon})T) \quad (1)$$

where σ is the plastic flow stress, $\dot{\varepsilon}$ is the strain rate, ε is the plastic strain, and T is the temperature. C_0 , B , β_0 , β_1 , B_0 , ε_r , α_0 , and α_1 are experimentally determined material constants for TRC wrought AZ31B and are listed in Table 1 (Ammouri and Hamade, 2013b). The coefficients were determined by fitting Eq. (1) to flow curves of TRC wrought AZ31B obtained from tensile tests at different temperatures and strain rates (Rodriguez et al., 2013).

The ZA constitutive relation was chosen due to its suitability for simulating friction stir processes according to a methodology recently proposed by the authors in Ammouri and Hamade (2014). This ZA relation accounts for strain hardening, strain rate hardening, and temperature softening as well as grain size. The term C_0 of Eq. (1) accounts for the contribution due to solutes and initial dislocation density along with the average grain diameter. The second and third terms of the equation are the constituents of the thermal stress component for bcc and fcc metals, respectively. When combined together, terms 2 and 3 describe the intermediate behavior of hcp material and are defined as the Peierls stress type interactions and intersection of forest dislocations type interactions (Zerilli and Armstrong, 1987).

2.3. Z-Parameter calculations

FSP process parameters used in the FE simulations are conducted according to the test matrix in Table 2 with tool rotational speeds and tool feed rates set at values ranging from 600 to 2000 rpm and from 75 to 900 mm/min, respectively. In the table, the nomenclature for the test cases are placed between parentheses and will be used to identify the test cells in the manuscript henceforth. The temperature and strain rate values for each test case were estimated from the FEA model and were used in the calculation of the Z-parameter.

The procedure for calculating the Z-parameter depends on the history of strain rate and temperature of 9 moving observation points placed in the FEA model. Fig. 2 illustrates the position of the observation points at different simulation time steps shown from the top view (Fig. 2a–c) and from the side view (Fig. 2d–f).

Figs. 3 and 4 show the temperature and strain rate histories, respectively, as the tool traverses across the observation points for the test cases A2 and H2, respectively. Test case A2 had a maximum temperature of $376 \pm 30^\circ\text{C}$ whereas test case H2 approached the melting point of Magnesium with a maximum temperature of $601 \pm 35^\circ\text{C}$. The difference in time scales between test cases A2 and H2 is due to the different feed rates of the considered test cases with a 100 mm/min for test case A2 and 700 mm/min for test case H2. The maximum reported average strain rate for test cases A2 and H2 were $34.8 \pm 5.2 \text{ s}^{-1}$ and $122.5 \pm 11.2 \text{ s}^{-1}$, respectively. The ratio between the maximum reported strain rate for cases H2 and A2 is around 3.5 which corresponds to the same ratio of the tool rotational speeds of these test cases (2000 rpm and 600 rpm).

For each simulation time step the values of the temperature and strain rate of the 9 observation points are compared against the reported limits of DRX identified according to Darras (2008) as temperature and strain rate values exceeding 227°C and 0.5 s^{-1} , respectively. The values of the Z-parameter are updated only if the recrystallization limits are exceeded. This procedure was applied to the 24 cases of the test matrix and the calculated linear average over the 9 observation points of Z are shown in Fig. 5a which reports calculated values of $\ln(Z)$ with corresponding values of Z in the range of $7.4\text{e}11$ – $2.7\text{e}13$.

Table 1
Fit coefficients for ZA of TRC wrought AZ31B.

C_0	B	β_0	β_1	B_0	ε_r	α_0	α_1
0	590	$3.6e-3$	$3.6e-5$	653	0.089	$6.1e-4$	$1.7e-4$

Table 2
The matrix used in FE simulations (symbols between parentheses are test cells' notation).

Tool rotational speed, rpm							
600	800	1000	1200	1400	1600	1800	2000
Feed rate, mm/min							
75 (A1)	100 (B1)	100 (C1)	150 (D1)	300 (E1)	350 (F1)	400 (G1)	500 (H1)
100 (A2)	125 (B2)	150 (C2)	250 (D2)	500 (E2)	550 (F2)	600 (G2)	700 (H2)
125 (A3)	150 (B3)	200 (C3)	350 (D3)	700 (E3)	750 (F3)	800 (G3)	900 (H3)

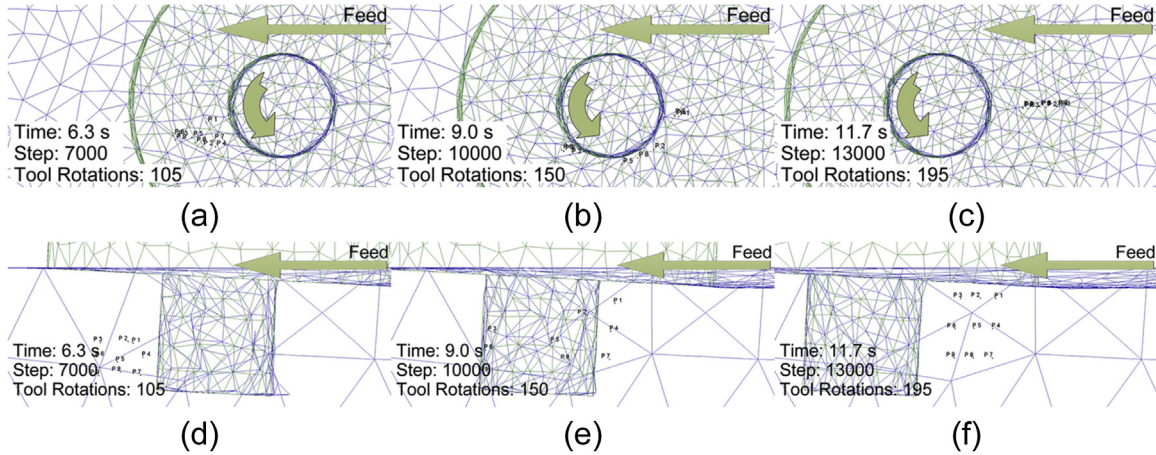


Fig. 2. Tracked points history for test case C1 for simulation steps 7000, 10,000, and 13,000 shown from the top view (a, b, and c) and from the side view (d, e, and f), respectively.

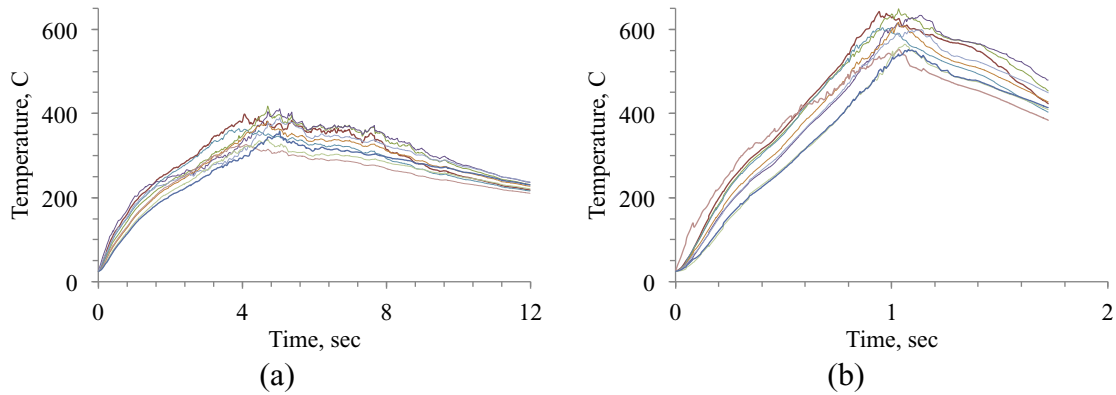


Fig. 3. Tracked temperature history for the 9 moving observation points for (a) test case A2 and (b) test case H2.

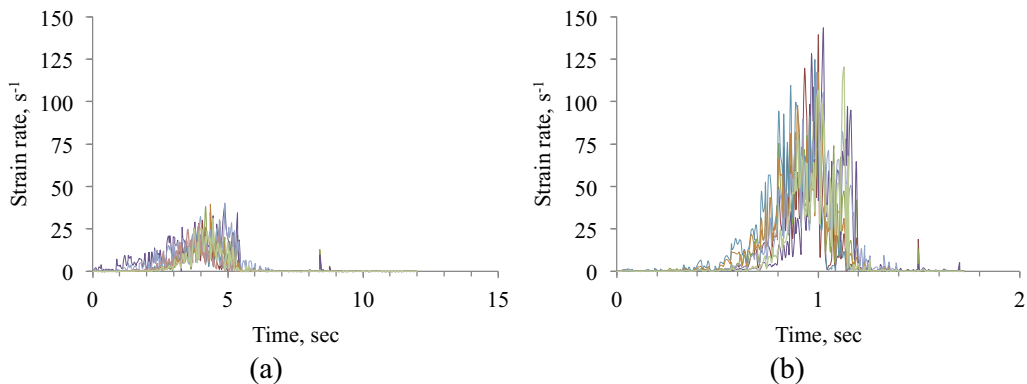


Fig. 4. Tracked strain rate history for the 9 moving observation points for (a) test case A2 and (b) test case H2.

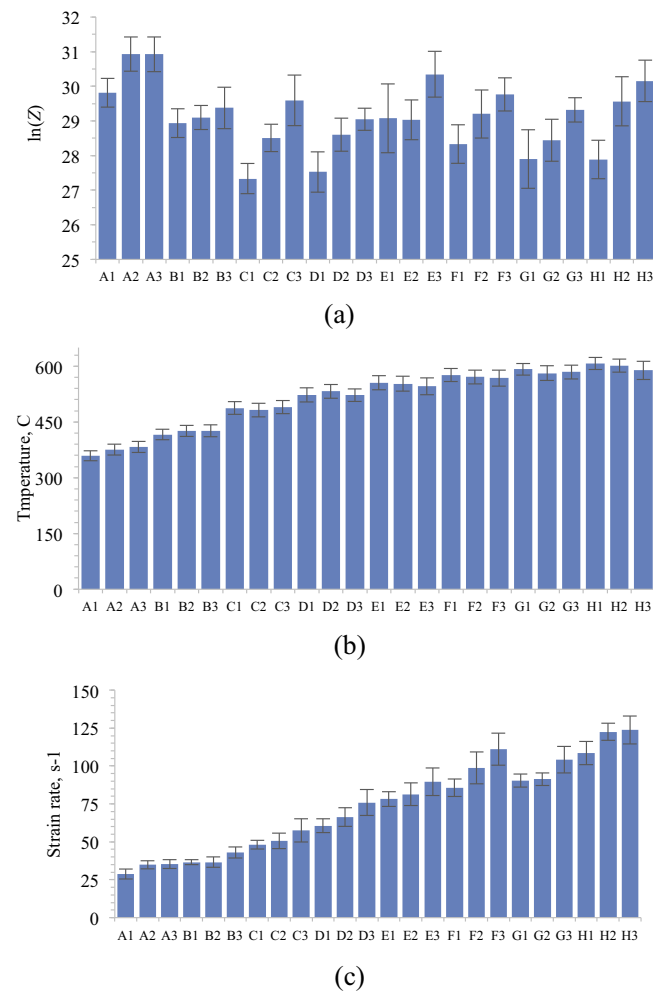


Fig. 5. Summary of (a) $\ln(Z)$, (b) maximum temperature, and (c) maximum strain rate for the 24 cases of the test matrix in Table 2. Variation spread bars show the variations in the $\ln(Z)$ values calculated at 9 observation points.

It can be noticed from Fig. 5a that $\ln(Z)$ increases with increasing feed rate for constant rotational speed. Furthermore, an overall decreasing $\ln(Z)$ trend can also be noticed for increasing tool rotational speed which is due to the coupled effect of increased strain rate and temperature. Fig. 5b and c shows the corresponding maximum temperature and the maximum observed strain rate, respectively, for different cases as predicted by the FE simulations. For cases with constant rpm with increasing feed rate, it is observed that the resulting temperature is almost constant while the strain rate increases, hence the increase of $\ln(\dot{\epsilon})$ leads to an increase of $\ln(Z)$. However and as both temperatures and strain rates evolve, the component that contributes more to Z-parameter evolution is attributed to second term of the equation $\ln(Z) = \ln(\dot{\epsilon}) + (Q + RT)$ leading to overall decrease in values of $\ln(Z)$.

Variation spread bars show the variations in the calculated $\ln(Z)$ values for the 9 observation points. This variation spread comes about from averaging the values at the 9 observation points which are located at different heights throughout the thickness resulting in variation of $\pm 3\%$ indicates relatively small variations in the values of the Z-parameter across plate thickness.

3. Experimental verification

In this section, conducted are experimental verifications of the FEA results reported in Section 2.

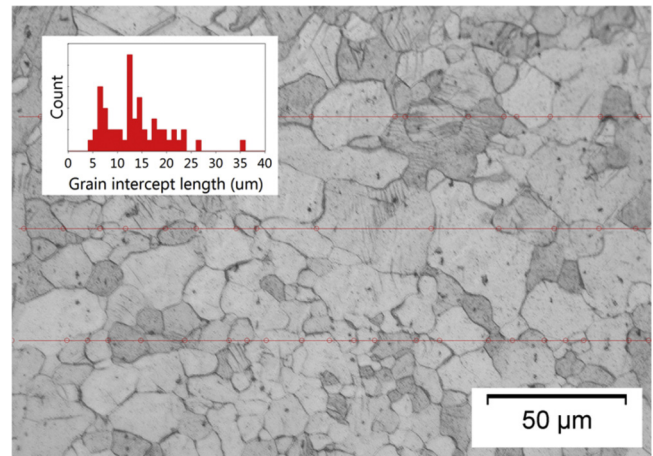


Fig. 6. As received microstructure of TRC AZ31B at $50\times$ magnification.

3.1. Experimental setup

Friction stir processing was performed on 3-mm-thick sheets of twin-roll cast (TRC) AZ31B magnesium alloy in the as-twin-rolled received condition. The chemical composition of the material (POSCO, 892 Gaechi4-dong, Gangam-gu, Seoul, 135-777) was obtained through energy dispersive X-ray analysis (EDX). Material composition by weight percentage was: Mg 95.4%, Al 3.32%, Zn 0.803%, Mn 0.304%, and Si 0.147% (Rodriguez et al., 2013).

Single pass FSP was performed on a HAAS VF6 vertical machining center which was retrofitted with external hardware to perform friction stir processes (for experimental details see Kheireddine et al., 2013). The workpiece fixture consists of a C30 steel backing plate and two holders. A 2 mm deep groove was machined in the backing plate to hold the workpiece. The workpiece is mounted on the backing plate and two holders made from the same C30 steel are used to firmly hold the workpiece. The FSP tool is machined from SVERKER 21 (aka AISI-D2) tool steel supplied by Uddeholms AB (SE-683 85 Hagfors, Sweden). The tool was hardened after machining. The square tool has a shoulder diameter of 19 mm and straight pin that is 2.7 mm high and diameter of 6.4 mm.

FSP was performed on each of the test matrix cases of Table 2. The samples were then cut, ground, polished, and etched using Acetic-Picral solution according to the ASM Specialty Handbook of Magnesium and Magnesium Alloys. Microstructure images were taken using a B41 Olympus microscope equipped with an Olympus XC50 digital camera. Fig. 6 shows a typical sample in the as-received condition material microstructure at $50\times$ magnification. The material is characterized by non-uniform grain sizes varying from 4.3 to $41.2\mu\text{m}$ with an average grain size of $15.3\mu\text{m}$ (measured according to ASTM E112-10). Grain size measurements were performed along the center line of the FSP pass just beneath the top surface, several micrographs have been taken along this line and the average grain size for each case calculated.

3.2. Experimental results

Optical observations of the friction stir processed samples were characterized by refined, equi-axial grain distribution as seen by micrographs of six different test cases in Fig. 7 with the degree of grain refinement varies with processing parameters. Statistical results for these 6 micrographs considered in Fig. 7 are listed in Table 3. Rodriguez et al. (2013) reported that the resultant grain size is the consequence of a competition between grain refinement, due to increasing strain rate, and grain growth, due to the heat input.

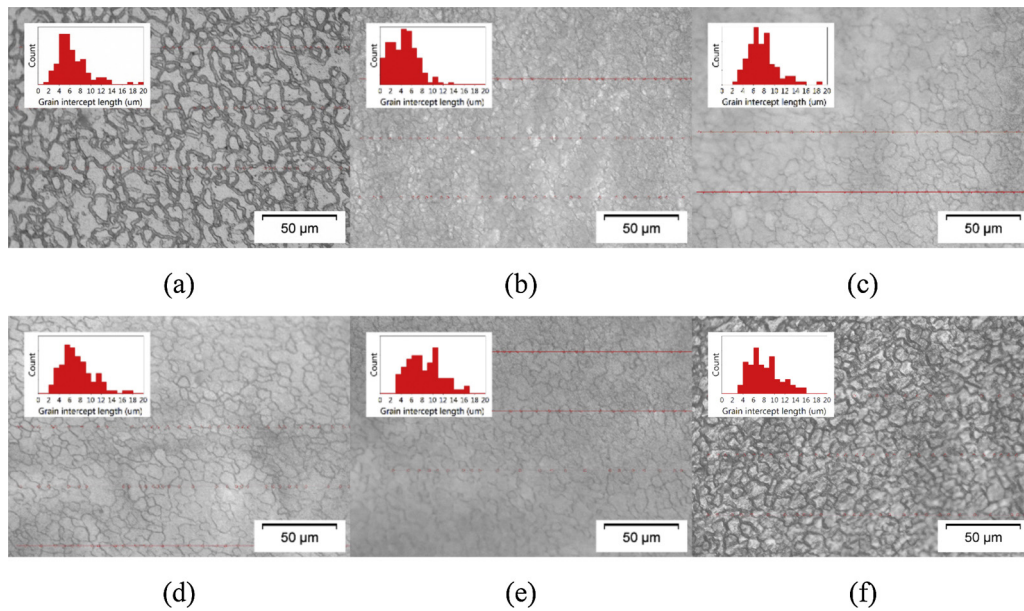


Fig. 7. Optical micrographs with 50× magnification showing histogram of grain intercept length of processed test cases (a) A1, (b) A3, (c) C3, (d) D3, (e) F2, and (f) G3.

Table 3

Statistical data for the grain size of AZ31B shown in micrographs of Fig. 7. Also listed for comparison are grain size data for as-received material (Fig. 6).

Test case	A1	A3	B1	B3	C1	C3	D1	D3
Average grain size, μm	6.6	5.4	9.1	8.5	9.6	6.4	12.8	7.7
Test case	E1	E3	F1	F3	G1	G3	H1	H3
Average grain size, μm	9.1	6.5	8.0	6.5	9.6	7.7	10.2	7.0

Table 3 shows that for cases with constant rpm and an increasing the feed rate, the grain size is decreased as the temperature is almost constant and the strain rate is increased. However, for cases with fairly constant strain rate and increasing temperatures (E3,G1; A3,B1; F3,H1), an increase in the average grain size is noticed. The grain size obtained by combining a heat input and strain rate increase (by increasing the tool rpm and feed rate) will result from the two competing phenomenon described above. Therefore, the Z-parameter is a suitable variable that can be used to describe the combined effect of strain rate and temperature on grain size.

4. Grain size vs. Z-parameter

Plotting the values of $\ln(Z)$ obtained from the experimentally validated FE model (such as those in Fig. 7) against the natural logarithm of the experimentally calculated average grain size values (Table 3) yields the plot in Fig. 8. A linear trendline of the average grain size values vs. Z-parameter trends yields ($R^2 = 0.887$) the newly found relation

$$\ln d = -0.23 \ln Z + 8.79 \quad (2)$$

For contrast, the previously reported trends for AZ31 by Chang et al. (2004) and Darras (2008) are co-plotted in Fig. 8. The plot shows practically parallel trends with the value of the coefficient a found in this work to be -0.23 compared with -0.27 in Chang et al. (2004) and -0.21 in Darras (2008).

For AZ31B, Fig. 8 suggests that, a linear relation relates the evolution of the average grain size in function of the Z-parameter, in natural logarithmic scale. For the different data, the difference in the parameters of this linear relation can be attributed to the processing condition of the as-received materials. Processing of

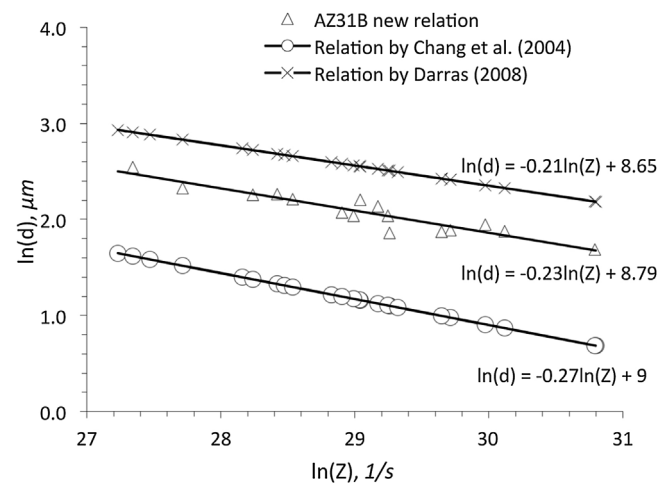


Fig. 8. The newly introduced grain size relation for the TRC AZ31B. Co-plotted for comparison are relations obtained by Chang et al. (2004) and by Darras (2008).

the as-received material induce internal stresses that influence the kinetics of dynamic recrystallization. Furthermore, the initial grain size of the as-received material influences the kinetic of dynamic recrystallization. It is also widely recognized that the deformation mechanisms are affected by grain size and orientation (texture). For example, Dogan et al. (2014) reported that the relative activity of twinning decreases with decreasing grain size. Also, Young et al. (2014) reported that reducing twinning at room temperature contributes to decreasing the ductility (with ductility increasing at higher temperatures). Deformation by twinning is reported to be one of the main mechanisms contributing to dynamic recrystallization. A thorough future study of the effect of the initial

microstructure on the resulting grain size by FSP would be needed to thoroughly explain the trend lines in Fig. 8 in a unified manner.

5. Conclusions

Determined in this work are coefficients for the relation in (2) which describes the variation of the average grain size with the Z-parameter for twin roll cast AZ31B magnesium alloy resulting from friction stir processing. An experimentally validated FE model was used to calculate the Z-parameter for a wide range of process parameters: spindle speed of 600–2000 rpm and tool feed rates of 75–900 mm/min. The average grain size was determined experimentally from the micrographs of the friction stir processed samples. It was found that the newly determined coefficients a and b of the relation were -0.23 and 8.79 , respectively. When compared to previously reported values for AZ31B plates extruded from square billets by Chang et al. (2004), the values of a and b coefficients were off by 17.4% and 2.4% respectively. This is attributed to the different material preparation technique used to prepare the sheets (billet by Chang et al. (2004) vs. TRC here) which would result in different as-received micro structure. Comparing the newly determined a and b coefficients with those obtained for AZ31B-O annealed as-received sheets by Darras (2008), the values were slightly off by 8.7% and 1.6%, respectively.

Acknowledgments

This publication was made possible by the National Priorities Research Program (NPRP) grant # 09-611-2-236 from the Qatar National Research Fund (a member of The Qatar Foundation). The statements made herein are solely the responsibility of the authors. Hamade and Ammouri also acknowledge the support of the University Research Board (URB) of the American University of Beirut (AUB).

References

- Ammouri, A.H., Kheireddine, A.H., Kridli, G.T., Hamade, R.F., 2013. FEM optimization of process parameters and in-process cooling in the friction stir processing of magnesium alloy AZ31B. Proceedings of the ASME International Mechanical Engineering Congress and Exposition, IMECE 2013, 15–21 November 2013, San Diego, California, USA.
- Ammouri, A.H., Hamade, R.F., 2013a. A relation between grain size and process parameters in friction stir processing of AZ31B. *Int. J. Appl. Eng. Res.* 8, 977–982.
- Ammouri, A.H., Hamade, R.F., 2013b. Comparison of material flow stress models towards more realistic simulations of friction stir processes of Mg alloy. *Adv. Mater. Res.* 922, 18–22.
- Ammouri, A.H., Hamade, R.F., 2014. On the selection of constitutive equation for modeling the friction stir processes of twin roll cast wrought AZ31B. *Mater. Des.* 57, 673–688.
- Chang, C., Lee, C., Huang, J., 2004. Relationship between grain size and Zener–Holloman parameter during friction stir processing in AZ31 Mg alloys. *Scr. Mater.* 51, 509–514.
- Chang, C., Du, X., Huang, J., 2007. Achieving ultrafine grain size in Mg–Al–Zn alloy by friction stir processing. *Scr. Mater.* 57, 209–212.
- Chang, C., Du, X., Huang, J., 2008. Producing nanogained microstructure in Mg–Al–Zn alloy by two-step friction stir processing. *Scr. Mater.* 59, 356–359.
- Darras, B., Khraisheh, M., Abu-Farha, F., Omar, M., 2007. Friction stir processing of commercial AZ31 magnesium alloy. *J. Mater. Process. Technol.* 191, 77–81.
- Darras, B.M., 2008. Integrated Thermo-Mechanical Investigations of Friction Stir Processing of Light Weight Alloys, PhD Theses. University of Kentucky.
- Dogan, E., Karaman, I., Ayoub, G., Kridli, G., 2014. Reduction in tension-compression asymmetry via grain refinement and texture design in Mg-2Al-1Zn sheets. *Mater. Sci. Eng. A* 610, 220–227.
- Friedrich, H., Schumann, S., 2001. Research for a “new age of magnesium” in the automotive industry. *J. Mater. Process. Technol.* 117, 276–281.
- Kheireddine, A.H., Ammouri, A.H., Kridli, G.T., Hamade, R.F., 2013. Experimentally validated thermo-mechanically coupled FE simulations of Al/Mg friction stir welded joints. In: Proceedings of the ASME International Mechanical Engineering Congress and Exposition, IMECE 2013, 15–21 November 2013, San Diego, California, USA.
- McQueen, H.J., Myshlaev, M., Sauerborn, M., Mwembela, A., 2000. Flow stress microstructures and modeling in hot extrusions of magnesium alloys. In: Kaplan, H.I., Hryn, J.N., Clow, B.B. (Eds.), *Magnesium Technology*. The Minerals, Metals and Materials Society, Warrendale, PA, pp. 355–362.
- Mishra, R.S., Mahoney, M.W., 2001. Friction stir processing: a new grain refinement technique to achieve high strain rate superplasticity in commercial alloys. *Mater. Sci. Forum* 357, 507–514.
- Rodriguez, A.K., Kridli, G., Ayoub, G., Zbib, H., 2013. Effects of the strain rate and temperature on the microstructural evolution of twin-rolled cast wrought AZ31B alloys sheets. *J. Mater. Eng. Perform.* 22, 3115–3125.
- Young, J.P., Ayoub, G., Mansoor, B., Field, D.P., 2014. The effect of hot rolling on the microstructure, texture and mechanical properties of twin roll cast AZ31Mg. *J. Mater. Process. Technol.* 216, 315–327.
- Wang, Y., Lee, C., Huang, C., Lin, H., Huang, J., 2003. Influence from extrusion parameters on high strain rate and low temperature superplasticity of AZ series Mg-based alloys. *Mater. Sci. Forum* 426, 2655–2660.
- Zerilli, F.J., Armstrong, R.W., 1987. Dislocation-mechanics-based constitutive relations for material dynamics calculations. *J. Appl. Phys.* 61, 1816–1825.
- Zerilli, F.J., 2004. Dislocation mechanics-based constitutive equations. *Metall. Mater. Trans. A* 35, 2547–2555.